Experimental $P-T-\rho$ Measurements of Supercritical Mixtures of Carbon Dioxide, Carbon Monoxide, and Hydrogen and Semiquantitative Estimation of Their Solvent Power Using the Solubility Parameter Concept

Andrea Cipollina, Rosalba Anselmo, Onofrio Scialdone, Giuseppe Filardo, and Alessandro Galia*

Dipartimento di Ingegneria Chimica dei Processi e dei Materiali, Università di Palermo, Viale delle Scienze Ed. 6, 90128 Palermo, Italy

The $P-T-\rho$ behavior of the CO_2-CO-H_2 system was studied in the supercritical region under operative conditions close to those adopted to perform hydrogenation and hydroformylation reactions in dense CO_2, thus providing new interesting information on this fluid mixture. Experiments were performed in a fixed volume reactor in the temperature range from 298 K to 343 K changing the density and the composition of the fluid phase. The one-component (Hildebrand) solubility parameter of the mixture was estimated from experimentally measured *P* vs *T* profiles, and its dependence on the density and composition of the system was analyzed to study the antisolvent effect of the permanent gases. We have found that, under adopted operative conditions, the Peng−Robinson equation of state (PR-EOS) can be used to predict with good accuracy the values of the Hildebrand solubility parameter of the binary and ternary mixtures without using adjustable binary interaction parameters. The PR-EOS was eventually used to calculate the dependence of the solubility parameter of CO_2-containing mixtures on the composition, pressure, and density. By this approach, it seems that the antisolvent effect of CO and H_2 is mainly due to the reduction of the density of the fluid phase, at fixed *T* and *P*, when the mole fraction of *syn*-gas components is increased.

Introduction

In the last two decades, the interest in the utilization of supercritical carbon dioxide ($scCO_2$) as a reaction medium has greatly increased because of the interesting environmental, health and safety, process, and chemical benefits that can be obtained when it is used in several synthetically useful chemical reactions.[1] In particular, when gaseous reagents are involved, as in the case of homogeneously catalyzed hydrogenation and hydroformylation reactions, the adoption of $scCO_2$ as an alternative to liquid solvents can allow the operator to perform the reaction under single-phase conditions thus increasing the local concentration of the dissolved gases and markedly accelerating the mass transfer kinetics both for the elimination of the gas−liquid interphase and for the better transport properties of supercritical fluids in comparison with liquid solvents. These benefits can be attenuated or even vanified by the limited solubility of conventional homogeneous catalytic systems in $scCO_2$. This problem can be further complicated when low critical temperature gaseous reagents are involved, as it has been observed that the solvent power of CO_2 is progressively reduced when the mole fraction of permanent gases loaded in the system increases. This effect has been clearly observed in the case of nitrogen and helium.[2,3]

For these reasons, the need arises for characterization of the $P-T-\rho$ behavior of CO_2-*syn*-gas mixtures at supercritical conditions, collecting novel experimental data to validate a simple EOS that can become a precious tool to predict the properties of these mixtures under different operating conditions in the perspective of industrial utilization.

In the present work, pressure, temperature, and density relations have been experimentally measured for several fluid mixtures containing CO, H_2, and CO_2 at different compositions. Such data were used to estimate the Hildebrand solubility parameter[4] of the mixture under adopted experimental conditions, as this concept, even if originally defined for condensed systems, has also been proposed as a useful indicator of the solvent power of supercritical fluids.[5]

The regular solution theory approach, even if only semiquantitative in the description of the mixture, can be useful also as a rough guide to orient molecular design of ligands because it has been observed that experimentally measured mole fraction solubility of copper(II) and chromium(III) β-diketonates in $scCO_2$ can be correlated with the solubility parameter of the free ligand.[6]

The Peng−Robinson equation of state (PR-EOS) has been tested to fit experimental points and to be used as a predictive tool for a more complete description of the dependence of the solubility parameter on composition, temperature, and pressure of the fluid system.

Materials and Experimental Apparatus

Hydrogen and carbon dioxide were purchased from AirLiquid with a purity of 99.999 % and 99.998 %, respectively. Carbon monoxide was supplied by Sapio with a reported purity of 99.0 %.

Experiments were performed in a stainless steel reactor with a volume of 28.5 ± 0.1 mL (determined by several measurements with $scCO_2$ and Ar at different masses, pressures, and temperatures) designed to operate up to 60 MPa. The pressure vessel was equipped with a pressure transducer (Barksdale UPA3) (estimated accuracy by calibration with a high-precision manometer is ± 0.05 MPa) and a Pt100 temperature sensor (estimated accuracy of ± 0.3 K). Both temperature and pressure

* Corresponding author. E-mail: galia@dicpm.unipa.it.

10.1021/je700307r CCC: $37.00
Published on Web 09/29/2007

inside the reactor were monitored in real time by a National Instrument acquisition board.

Experimental P vs T profiles were obtained by submerging the reactor in an electronically controlled thermostatic bath described elsewhere.[7] The vessel was heated from 298 K to 343 K and then cooled between the same temperatures. Both thermal paths were obtained by a progression of stepwise increases of temperature having an amplitude of 5 K; each experimental point was recorded after the equilibrium was achieved, as detected from the invariance of the recorded values of the intensive parameters.

The procedure for pressurizing the reactor started with the determination of its mass. Air was then removed by purging at least three times with gaseous hydrogen or carbon monoxide at a pressure lower than 5 MPa. Then, H_2 and/or CO were dosed by adjusting their partial pressure while the reactor was immersed in a thermostatic bath at (283 ± 1) K. For this purpose, a Tescom pressure reducer connected to both storage vessels through a suitable valve system was used. When present, hydrogen was always delivered first to estimate its mass from temperature and pressure readings using the PR-EOS with effective critical parameters (vide infra), after having tested the accuracy of the EOS using $P-T-\rho$ NIST data on pure hydrogen. With such a procedure, the experimental error was estimated to be less than ± 0.004 g. The total mass of CO loaded was measured gravimetrically by an electronic balance with an accuracy of ± 0.01 g. The last component introduced was liquid CO_2 delivered by means of a Maximator air-driven pump until the final selected pressure was reached. Before charging each compound, the corresponding lines were always carefully purged, and back flows were prevented by keeping CO and CO_2 lines at higher pressure than that inside the reactor. The total mass of loaded components was then measured. This value was used to determine the amount of delivered carbon dioxide (uncertainty of ± 0.01 g) and the density of the mixture. Mass and molar fractions were then calculated, and with the aforementioned uncertainties in the values of the mass of each component, the uncertainty in the mole fractions of the gaseous components was estimated to be lower than 0.005.

The pressurized vessel was submerged in the thermostatic bath, and the experimental run was started according to the procedure previously described. A sketch of the experimental apparatus has been reported elsewhere.[7]

Peng−Robinson EOS

The Peng−Robinson equation of state[8] belongs to the family of semiempirical cubic EOSs, and it has been frequently used to model the phase behavior of fluid mixtures at supercritical conditions with good accuracy.[3,9−11]

The PR-EOS can be written in the following form

$$P = \frac{RT}{v-b} - \frac{a}{v(v+b)+b(v-b)} \tag{1}$$

In the case of a pure component, the two parameters a and b are related to the critical properties by the equations

$$a = 0.45724\,\frac{R^2T_c^2}{P_c}\alpha(T_r,\omega) \tag{2}$$

$$b = 0.0778\,\frac{RT_c}{P_c} \tag{3}$$

Table 1. Critical Properties of the Three Mixture Components

component		T_c/K	P_c/MPa	ω
1	CO_2	304.1	7.38	0.239
2	CO	132.9	3.50	0.066
3	H_2[a]	43.6	2.05	0.000

[a] All parameters taken from ref 12. In the case of hydrogen, high-temperature effective critical properties have been used.

The dependence of dimensionless function α on the reduced temperature T_r and the acentric factor ω is expressed by the following equation

$$\alpha = [1 + (0.37464 + 1.54226\omega - 0.26992\omega^2)(1 - T_r^{1/2})]^2 \tag{4}$$

In the case of mixtures, the same eq 1 can be used, provided that parameters a and b of the mixture are defined by suitable mixing rules. The following van der Waals mixing rules were used in the original article of Peng and Robinson and have been adopted in this study

$$a = \sum_i \sum_j x_j x_i a_{ij} = \sum_i x_i^2 a_i + \sum_{i\neq j} x_i x_j a_{ij} \tag{5}$$

$$b = \sum_i x_i b_i \tag{6}$$

$$a_{ij} = (1 - k_{ij}) a_i^{1/2} a_j^{1/2} \tag{7}$$

where k_{ij} is an empirically determined binary interaction coefficient characterizing each pair of components of the mixture.

The pure component parameters used in the PR-EOS are listed in Table 1. Because of its small molecular mass, the configurational properties of hydrogen, like those of helium and neon, are described by quantum rather than classical statistical mechanics. For this reason, acentric factors of such "quantum gases" are slightly negative and physically not significant. Corresponding-state correlations for virial coefficients may also be applied to these molecules by using the so-called effective critical constants and $\omega = 0$.[12] Even if the parameters change with temperature, corrections are not important at room or higher temperatures and "classical" values extrapolated at very high absolute temperature can be used. This approach has already been adopted to describe the antisolvent effect of helium dissolved in $scCO_2$.[3] The same choice has been made in this work, as the $P-T-\rho$ data of pure H_2 taken from the NIST database, in the temperature and pressure range adopted in the present study, have been better correlated using the high-temperature effective parameters rather than real critical parameters with $\omega = -0.216$ (see Supporting Information).

Hildebrand Solubility Parameter of the Mixture

The concept of solubility parameter was originally defined for regular solutions by Hildebrand and Scott and has been widely used to correlate and predict the solubility behavior of two components based on the knowledge of the individual components alone.[13] This concept has been frequently used to qualitatively correlate the solvent power of supercritical fluids.[2,3,14]

For nonpolar/nonassociating fluids or polar fluids with a dipole moment lower than 2 D (1 D is equal to $3.336\cdot10^{-30}$ C·m), the cohesive energy density ($\Delta U/v$) can be approximated by the internal pressure $(\partial U/\partial v)_T$ that can be calculated from a thermodynamic EOS[15]

$$\delta = \left(\frac{\Delta U}{v}\right)_T^{1/2} \approx \left(\frac{\partial U}{\partial v}\right)_T^{1/2} = \left[T\left(\frac{\partial P}{\partial T}\right)_v - P\right]^{1/2} \quad (8)$$

In the system under consideration, both CO_2 and H_2 are nonpolar gases, whereas CO has a dipole moment of 0.112 D ($3.74 \cdot 10^{-31}$ C·m) and can, therefore, be assumed a nonpolar gas too.[15] From eq 8, it can be inferred that one component solubility parameter of a dense gaseous mixture can be estimated from the P vs T profiles recorded in a fixed volume reactor. Some typical experimental profiles obtained in this study are reported in Figure 1. The experimental points can be excellently fitted by straight lines, and for this reason, the last term in eq 8 corresponds to the square root of the modulus of intercepts.

Experimentally estimated values of the solubility parameter can be compared with those obtained using an EOS to analytically express the last term in eq 8. Using the PR-EOS, the term in the square brackets in eq 8 can be written under the form

$$T\left(\frac{\partial P}{\partial T}\right)_v - P = -\frac{T}{v(v+b)+b(v-b)}\cdot\frac{\partial a}{\partial T} + \frac{a}{v(v+b)+b(v-b)} = \frac{1}{v(v+b)+b(v-b)}\left(a - T\frac{\partial a}{\partial T}\right) \quad (9)$$

In the case of a mixture, using Van der Waals mixing rules (eq 5), the partial derivative in eq 9 can be expressed by the equation

$$-T\frac{\partial a}{\partial T} = \sum_i x_i^2 a_i \frac{m_i\sqrt{\frac{T}{T_{c,i}}}}{1 + m_i\left(1 - \sqrt{\frac{T}{T_{c,i}}}\right)} + \sum_{i\neq j} x_i x_j a_{ij}\left[\frac{1}{2}\frac{m_i\sqrt{\frac{T}{T_{c,i}}}}{1 + m_i\left(1 - \sqrt{\frac{T}{T_{c,i}}}\right)} + \frac{1}{2}\frac{m_j\sqrt{\frac{T}{T_{c,j}}}}{1 + m_j\left(1 - \sqrt{\frac{T}{T_{c,j}}}\right)}\right] \quad (10)$$

where $m_i = 0.37464 + 1.54226\omega_i - 0.26992\omega_i^2$.

The solubility parameter can be analytically expressed by eq 11.

In the present work, this equation has been used to predict the solubility parameter of the mixture taking the value of the interaction parameters $k_{ij} = 0$.

Results and Discussion

Selection of the Value of Binary Interaction Parameters. Experiments were performed to collect P vs T profiles for several different binary mixtures, H_2-CO_2, $CO-CO_2$, and H_2-CO. Such data are reported in Tables 2 to 4 together with the values of densities. The latter were computed from the masses of loaded components, estimated as previously described, and from the value of the volume of the pressure vessel. All these data were used to evaluate the accuracy of the PR-EOS in the prediction of the volumetric behavior of the mixtures without using adjustable binary interaction parameters.

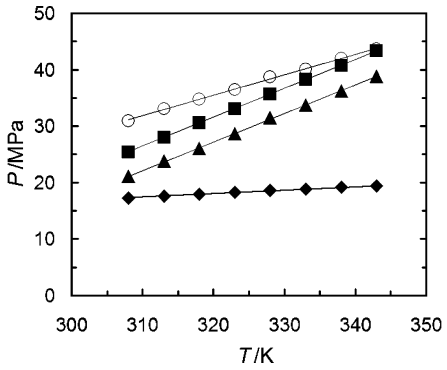

Figure 1. Typical experimental pressure P vs temperature T profiles of binary and ternary mixtures of CO_2, CO, and H_2: ○, system CO_2-CO-H_2, mixture 5 in Table 6; ■, system CO_2-CO, mixture 4 in Table 2; ▲, system CO_2-H_2, mixture 5 in Table 3; ◆, system $CO-H_2$, mixture 3 in Table 4.

Table 2. Experimental Pressure P as a Function of Temperature T and Experimental Density ρ for Mixtures of Carbon Dioxide (1) and Carbon Monoxide (2)

x_2	0.138	0.134	0.117	0.115	0.089	0.046	0.065
ρ/g·mL^{-1}	0.758	0.769	0.790	0.791	0.808	0.835	0.845
mix.	1	2	3	4	5	6	7
T/K				P/MPa			
308	26.0	26.6	25.5	25.4	24.7	22.5	26.5
313	28.0	29.1	28.4	28.0	27.2	25.4	29.6
318	30.5	31.6	30.7	30.6	30.2	28.3	32.2
323	32.8	34.1	33.6	33.1	32.7	31.3	35.2
328	35.2	36.6	36.2	35.7	35.5	33.9	38.1
333	37.4	39.1	38.9	38.3	37.9	36.6	41.1
338	39.9	41.6	41.6	40.8	40.8	39.4	44.1
343	42.3	44.1	44.4	43.3	43.0	42.2	47.0

Table 3. Experimental Pressure P as a Function of Temperature T and Experimental Density ρ for Mixtures of Carbon Dioxide (1) and Hydrogen (3)

x_3	0.244	0.130	0.138	0.135	0.045	0.065
ρ/g·mL^{-1}	0.461	0.624	0.728	0.748	0.795	0.819
mix.	1	2	3	4	5	6
T/K			P/MPa			
308	21.5	20.1	29.4	31.7	21.1	27.4
313	22.6	22.1	31.3	34.1	23.8	30.0
318	23.7	23.4	33.5	36.7	26.1	32.5
323	24.9	25.1	35.6	39.0	28.6	35.3
328	26.1	26.6	37.9	41.4	31.5	38.1
333	27.2	28.4	40.2	43.8	33.7	40.8
338	28.4	30.0	42.6	46.3	36.2	43.8
343	29.6	31.7	44.9	48.9	38.9	46.7

The experimental data of density and temperature of the different binary systems were used in the PR-EOS, assuming $k_{ij} = 0$, to predict the corresponding values of pressure. As a

$$\delta = \left\{\frac{\sum_i x_i^2 a_i\left[1 + \frac{m_i\sqrt{\frac{T}{T_{c,i}}}}{1 + m_i\left(1 - \sqrt{\frac{T}{T_{c,i}}}\right)}\right] + \sum_{i\neq j} x_i x_j a_{ij}\left[1 + \frac{1}{2}\cdot\frac{m_i\sqrt{\frac{T}{T_{c,i}}}}{1 + m_i\left(1 - \sqrt{\frac{T}{T_{c,i}}}\right)} + \frac{1}{2}\cdot\frac{m_j\sqrt{\frac{T}{T_{c,j}}}}{1 + m_j\left(1 - \sqrt{\frac{T}{T_{c,j}}}\right)}\right]}{v(v+b)+b(v-b)}\right\}^{1/2} \quad (11)$$

Table 4. Experimental Pressure *P* as a Function of Temperature *T* and Experimental Density ρ for Mixtures of Carbon Monoxide (2) and Hydrogen (3)

x_3	0.049	0.112	0.095	0.056	0.068	0.049
ρ/g·mL^{-1}	0.472	0.484	0.500	0.530	0.540	0.672
mix.	1	2	3	4	5	6
T/K	*P*/MPa					
308	8.8	20.6	17.3	10.9	13.0	12.6
313	8.9	21.0	17.6	11.1	13.2	12.9
318	9.1	21.3	17.9	11.3	13.4	13.0
323	9.3	21.7	18.2	11.5	13.7	13.2
328	9.4	22.1	18.6	11.7	13.9	13.5
333	9.6	22.4	18.8	11.8	14.1	13.7
338	9.7	22.8	19.2	12.0	14.3	13.9
343	9.9	23.1	19.4	12.3	14.6	14.1

Table 5. Effect of Interaction Parameters for the System CO_2 (1)−CO (2)−H_2 (3)

binary system	k_{ij}	ϵ/%	k_{ij}	ϵ/%
1−2	0	4.33	0.204	2.51
1−3	0	3.15	−0.112	2.94
2−3	0	2.37	0.429	2.23

comparison, a second approach was carried out using the binary interaction parameters as an adjustable quantity. In this case, the values of k_{ij} were determined forcing the value of density to those determined from the masses of loaded components (Tables 2 to 4) by minimizing the sum of the squared deviations between calculated and experimental pressure χ_P^2 for the whole set of points of each binary mixture

$$\chi_P{}^2 = \sum_{i=1}^{N} (P_i^{\text{calcd}} - P_i^{\text{exptl}})^2 \tag{12}$$

where N is the number of data points for each system; P_i^{exptl} is the observed pressure; and P_i^{calcd} is the analogous calculated quantity.

Table 5 reports the values of the percentage root-mean square deviation ϵ, defined in eq 13, for the values of the pressure obtained assuming null interaction parameters and with the k_{ij} optimized according to aforementioned criteria.

$$\epsilon = 100\sqrt{\frac{1}{N}\sum_{i=1}^{N}\left[\frac{(P_i^{\text{calcd}} - P_i^{\text{exptl}})}{P_i^{\text{exptl}}}\right]^2} \tag{13}$$

It can be observed that the adoption of adjustable binary interaction parameters does not significantly improve the precision of the PR-EOS in the prediction of the pressure of the mixtures at fixed T, ρ, and composition.

On this basis, we have decided to use the PR-EOS in a fully predictive manner assuming null binary interaction parameters for all couples of components.

The experimental data for different ternary mixtures of carbon oxides and hydrogen are summarized in Table 6 together with each mixture composition and experimental density.

A graphical representation of the deviations between calculated and experimental density values of all the investigated systems is reported in Figure 2. Using the PR-EOS without any adjustable parameters, deviations between calculated and experimental densities were always lower than 6 %, thus confirming that this cubic EOS can describe with good accuracy the volumetric behavior of CO_2−CO−H_2 systems.

Estimation of the Solvent Power of the CO_2−CO−H_2 System. The values of Hildebrand solubility parameters of binary and ternary mixtures containing carbon dioxide, obtained from

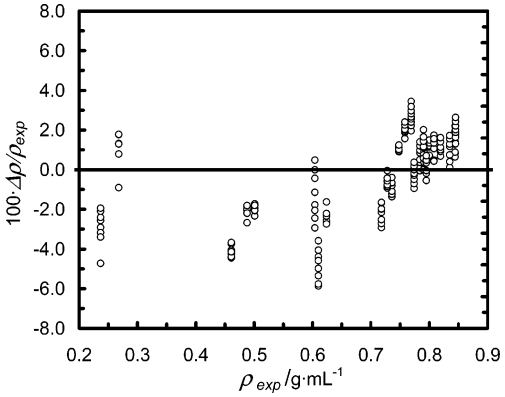

Figure 2. Discrepancy between density predicted by the PR-EOS and experimental data plotted vs experimental density for all CO_2-containing mixtures investigated in this work.

experimental P vs T profiles recorded in a fixed volume reactor, are reported in Table 7 together with the corresponding values calculated using eq 11.

In the case of systems containing hydrogen, we have found an excellent agreement between experimental and calculated δ with percentage differences lower than 3.2 % for most of the mixtures analyzed. Larger deviations were obtained in the case of binary mixtures of carbon oxides, but they were always lower than 6 % so that the agreement can be considered quite good. Moreover, calculations confirmed the experimental observation that changing the T at constant total density of the mixture negligibly alters the value of the Hildebrand parameter (Figure 3). From these results, it seems that the PR-EOS is a candidate not only to fit experimental data but also to analyze the effect of *syn*-gas on the solvent power of the fluid phase.

For this purpose, in Figures 4 and 5 are plotted the values of δ calculated using the cubic EOS for pure CO_2 and for selected mixtures having the same composition as those experimentally investigated in this study. A comparison was made by fixing the temperature at 333 K. It must be observed that, from the operative point of view, each profile corresponds to a fluid phase of fixed composition whose density is changed isothermally.

It can be immediately observed that, at fixed P, the addition of CO and/or H_2 to the supercritical solvent markedly decreases the value of δ and consequently the solvent power of the mixture. In particular, although for pure CO_2 δ varies from about (2.7 to 12.6) MPa$^{1/2}$ when pressure changes between (7 and 40) MPa, as also confirmed by literature data,[15] it varies from (1.6 to 7.3) MPa$^{1/2}$, in the same pressure domain, for mixtures containing about 0.2 mole fraction of H_2 and CO.

Interestingly, a similar behavior can be calculated for the change of density as a function of pressure when the mole fraction of low critical temperature gases added to the system is increased (Figures 6 and 7). Indeed, it is well-known that the solvent power of a supercritical fluid is mainly affected by its density, and this criterion seems respected also in the case of the ternary system under consideration. To verify in a more convincing way the aforementioned intuition, we have plotted again the values of δ against the values of densities of the mixtures. By this choice, a substantial overlapping of all the curves was obtained thus confirming that, in the range of investigated compositions, the main parameter affecting the solvent power of the fluid phase is the density (Figure 8).

This means that, on a first approximation, the antisolvent effect of CO and H_2 can be attributed to the reduction of the fluid density that occurs when molar fractions of these components at fixed T and P are increased. It must be observed

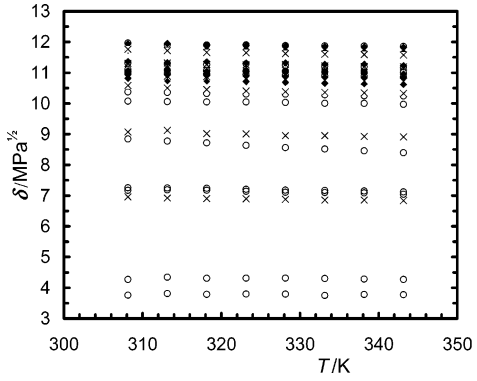

Figure 3. Effect of temperature on the calculated solubility parameters of mixtures investigated in this work under isochoric conditions: ○, ternary mixtures; ◆, CO_2−CO mixtures; ×, CO_2−H_2 mixtures.

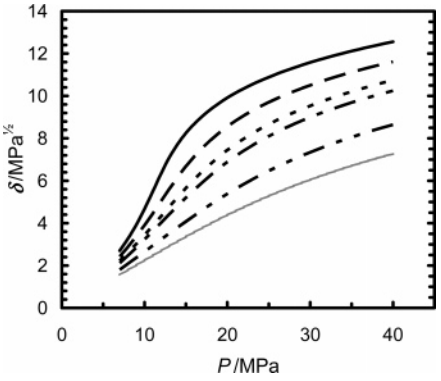

Figure 4. Hildebrand parameter vs total pressure for mixtures containing CO_2, CO, and H_2 at different molar fractions and $T = 333$ K: ——, pure CO_2; — —, $x_2 = 0.032$ and $x_3 = 0.035$; - - - -, $x_2 = 0.063$ and $x_3 = 0.063$; — · —, $x_2 = 0.074$ and $x_3 = 0.087$; — · · —, $x_2 = 0.132$ and $x_3 = 0.154$; ....., $x_2 = 0.204$ and $x_3 = 0.203$.

that this affirmation can be considered acceptable only if the cumulative molar fraction of the low critical temperature components is lower than a suitable threshold value.

In fact, if the trend of the Hildebrand parameter at $T = 333$ K is plotted against the *syn*-gas mole fraction, for the sake of simplicity assumed constituted by equimolar amounts of CO and H_2, for different values of constant densities (Figure 9), it can be easily observed that the solubility parameter can be significantly depressed, also keeping the density unchanged, when the mole fraction of CO and H_2 is high enough. In the same figure, we reported how pressure must be changed to keep the density constant when the mixture is depleted in carbon dioxide. It is evident that pressure increases steeply with the *syn*-gas mole fraction thus soon making the compensation of

Table 6. Experimental Pressure *P* as a Function of Temperature *T* and Experimental Density *ρ* for Mixtures of Carbon Dioxide (1), Carbon Monoxide (2), and Hydrogen (3)

x_2	0.074	0.212	0.124	0.204	0.132	0.049	0.072	0.023	0.063	0.070	0.032
x_3	0.087	0.240	0.120	0.203	0.154	0.069	0.049	0.065	0.063	0.018	0.035
ρ/g·mL^{-1}	0.237	0.268	0.488	0.501	0.604	0.718	0.736	0.774	0.784	0.800	0.844
mix.	1	2	3	4	5	6	7	8	9	10	11
T/K						*P*/MPa					
308	9.3	18.0	19.5	31.9	31.0	21.9	23.2	24.2	29.3	24.9	28.3
313	9.8	19.0	20.8	33.4	33.1	24.0	25.4	26.7	31.9	27.5	30.9
318	10.4	19.5	22.0	34.9	34.8	26.1	27.5	29.2	34.6	30.0	33.9
323	10.6	20.2	23.1	36.2	36.5	28.3	29.7	31.7	37.2	33.0	37.1
328	11.0	20.9	24.2	37.5	38.7	30.4	32.0	34.1	40.0	35.3	40.0
333	11.3	21.5	25.4	39.0	40.1	32.4	34.2	36.6	42.6	37.8	43.1
338	11.8	22.1	26.6	40.4	42.0	34.6	36.3	39.1	45.3	40.4	46.2
343	12.2	22.7	27.6	41.7	43.7	36.6	38.6	41.6	48.0	43.0	49.3

Table 7. Comparison of Experimental Solubility Parameters with Analogous Quantities Calculated with the PR-EOS for Different Ternary and Binary Mixtures Containing Dense Carbon Dioxide[a]

System CO_2 (1)−CO (2)							
x_2	0.138	0.134	0.117	0.115	0.089	0.046	0.065
ρ/g·mL^{-1}	0.758	0.769	0.790	0.791	0.808	0.835	0.845
mix.	1	2	3	4	5	6	7
δ^{exptl}/MPa$^{1/2}$	10.6	11.2	11.7	11.5	11.9	12.1	12.2
δ^{calcd}/MPa$^{1/2}$	10.7	10.9	11.0	11.0	11.3	11.7	11.9
$\lvert\Delta\delta/\delta\rvert$/%	0.4	3.0	5.7	4.0	4.6	2.9	2.4

System CO_2 (1)−H_2 (3)						
x_3	0.244	0.130	0.138	0.135	0.045	0.065
ρ/g·mL^{-1}	0.461	0.624	0.728	0.748	0.795	0.819
mix.	1	2	3	4	5	6
δ^{exptl}/MPa$^{1/2}$	6.9	8.9	10.1	10.7	11.4	11.8
δ^{calcd}/MPa$^{1/2}$	6.9	9.0	10.4	10.8	11.3	11.6
$\lvert\Delta\delta/\delta\rvert$/%	0.0	1.3	3.6	0.9	0.9	1.0

System CO_2 (1)−CO (2)−H_2 (3)											
x_2	0.074	0.212	0.124	0.204	0.132	0.049	0.072	0.023	0.063	0.070	0.032
x_3	0.087	0.24	0.12	0.203	0.154	0.069	0.049	0.065	0.063	0.018	0.035
ρ/g·mL^{-1}	0.237	0.268	0.488	0.501	0.604	0.718	0.736	0.774	0.784	0.800	0.844
mix.	1	2	3	4	5	6	7	8	9	10	11
δ^{exptl}/MPa$^{1/2}$	3.9	4.7	7.2	7.4	8.9	10.1	10.4	10.9	11.3	11.2	12.1
δ^{calcd}/MPa$^{1/2}$	3.8	4.3	7.1	7.2	8.6	10.1	10.3	10.9	11.1	11.2	11.9
$\lvert\Delta\delta/\delta\rvert$/%	3.0	8.5	1.0	2.8	3.2	0.7	0.9	0.2	2.2	0.4	1.7

[a] Numbering of mixtures is the same as that reported in Tables 2, 3, and 6.

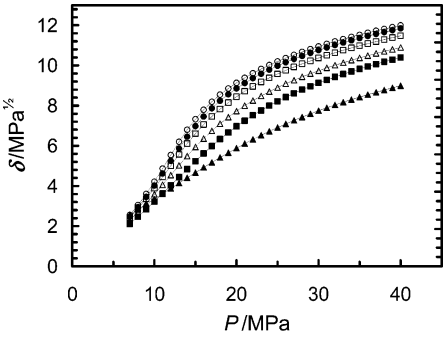

Figure 5. Hildebrand parameter vs total pressure for selected binary CO_2−CO (empty symbols) and CO_2−H_2 (filled symbols) mixtures at $T = 333$ K: ○, $x_2 = 0.046$; □, $x_2 = 0.089$; △, $x_2 = 0.138$; ●, $x_3 = 0.045$; ■, $x_3 = 0.135$; ▲, $x_3 = 0.244$.

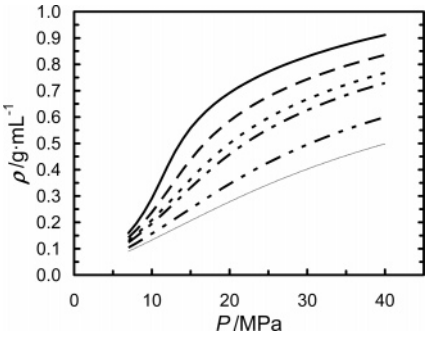

Figure 6. Density vs total pressure for mixtures containing CO_2, CO, and H_2 at different molar fractions and $T = 333$ K: ——, pure CO_2; — —, $x_2 = 0.032$ and $x_3 = 0.035$; - - - -, $x_2 = 0.063$ and $x_3 = 0.063$; — · —, $x_2 = 0.074$ and $x_3 = 0.087$; — · · —, $x_2 = 0.132$ and $x_3 = 0.154$; ....., $x_2 = 0.204$ and $x_3 = 0.203$.

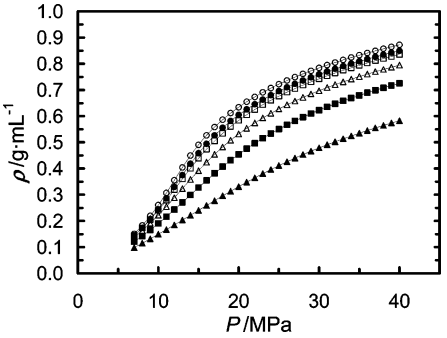

Figure 7. Density vs total pressure for selected binary CO_2−CO (empty symbols) and CO_2−H_2 (filled symbols) mixtures at $T = 333$ K: ○, $x_2 = 0.046$; □, $x_2 = 0.089$; △, $x_2 = 0.138$; ●, $x_3 = 0.045$; ■, $x_3 = 0.135$; ▲, $x_3 = 0.244$.

the aforementioned density reduction technically unpractical by increasing the working pressure.

These observations are very useful in the study of homogeneously catalyzed hydroformylation, hydrocarboxylation, and hydrogenation reactions. These processes are deeply investigated in $scCO_2$ also because the complete miscibility of CO and H_2 with CO_2 makes possible a significant enhancement of their concentration in the reaction medium. On the other hand, the problem of the limited solubility of conventional transition metal complexes must be faced to have the chance of concrete transfer of the technology from the laboratory to the industrial plant. A strategy to overcome this drawback is the design and synthesis of suitable CO_2-philic ligands that could act not only to optimize selectivity and activity of the metal center but also as solubilizing agents of the catalytic system in the fluid phase.

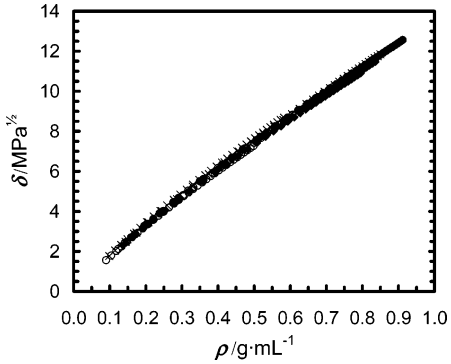

Figure 8. Hildebrand parameter vs density for different mixtures containing CO_2, CO, and H_2 at $T = 333$ K. ○, ternary mixtures: $x_2 = 0.032$ and $x_3 = 0.035$; $x_2 = 0.074$ and $x_3 = 0.087$, $x_2 = 0.204$ and $x_3 = 0203$. ◆, CO_2−CO mixtures: $x_2 = 0.089$, $x_2 = 0.138$. ×, CO_2−H_2 mixtures: $x_3 = 0.045$ and $x_3 = 0.244$.

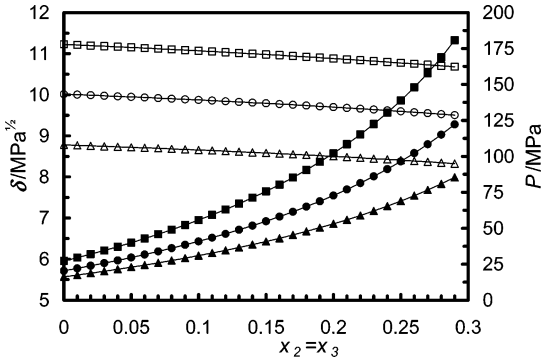

Figure 9. Plot of Hildebrand parameter (empty symbols) and of pressure (filled symbols) as a function of H_2 and CO mole fraction at $T = 333$ K and different mixture densities. ■, $\rho = 0.800$ g·mL^{-1}; ●, $\rho = 0.700$ g·mL^{-1}; ▲, $\rho = 0.600$ g·mL^{-1}.

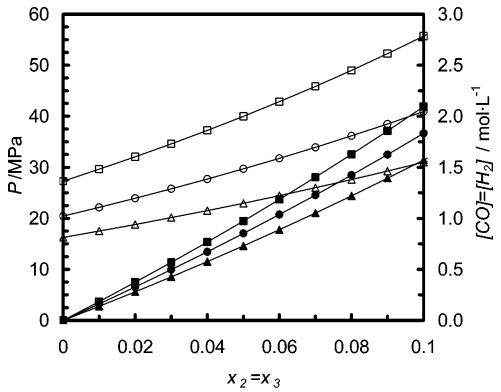

Figure 10. Plot of CO and H_2 molar concentration (filled symbols) as a function of their mole fraction at $T = 333$ K and different mixture densities. The trend of pressure (empty symbols) is also reported as a reference. ■, $\rho = 0.800$ g·mL^{-1}; ●, $\rho = 0.700$ g·mL^{-1}; ▲, $\rho = 0.600$ g·mL^{-1}.

In this scenario, it could be useful to have a first tentative criterion to predict the solubility behavior of the ligand in the reaction system from the knowledge of its behavior in pure carbon dioxide. From the results of this study, we can propose as a first approximation that the solubility of the species should be comparable provided that the total densities of the two fluid phases are similar. As previously highlighted, this criterion is valid only if the antisolvent mole fraction is low enough, and this could make its real utility questionable. For this reason, in Figure 10, we reported the curves to convert the concentration of H_2 and CO from the mole fraction scale to molar concentration for the same systems considered in Figure 9. We may observe that, in correspondence to mole fraction values of 0.1,

the maximum concentration of H_2 and CO in the fluid phase can be modified from 1.5 mol·L^{-1} to more than 2 mol·L^{-1} by changing the operating pressure from (30 to 55) MPa at 333 K thus indicating that the domain of applicability of the criterion covers the interval of concentrations of applicative interest.

Conclusions

Experimental data were collected on the $P-T-\rho$ behavior of supercritical mixtures of carbon dioxide, carbon monoxide, and hydrogen at different compositions. The effect of the two permanent gases was analyzed with respect to the fluid density ρ and the Hildebrand solubility parameter δ chosen as a semiquantitative estimation of the solvent power of the fluid phase. We have observed that both quantities are significantly decreased by increasing the molar fraction of H_2 and CO at constant T and P of the system, thus indicating an antisolvent effect of the *syn*-gas components. Quite interestingly, we have found that the values of ρ and δ can be predicted with good accuracy using the Peng−Robinson EOS (errors lower than 5 % in most cases) under a fully predictive form. It was moreover observed that the main factor determining the Hildebrand solubility value is the density of the fluid phase provided that the mole fractions of low critical temperature components are not too high.

Such a result can be interesting in the context of homogeneously catalyzed carbonylation and hydrogenation reactions in $scCO_2$, as it offers a first approximation criterion to estimate solubility of catalytic systems in the reaction system from their behavior in pure carbon dioxide.

Supporting Information Available:

Table with hydrogen density data from NIST compared with predictions of the PR-EOS using the two different sets of critical parameters. This material is available free of charge via the Internet at http://pubs.acs.org.

Literature Cited

(1) Jessop, P. G.; Leitner, W. *Chemical Synthesis Using Supercritical Fluids*; Wiley-VCH: Weinheim, 1999.

(2) King, J. W.; Zhang, Z. Selective extraction of pesticides from lipid-containing matrixes using supercritical binary gas mixtures. *Anal. Chem.* **1998**, *70*, 1431−1436.

(3) Roth, M. Helium head pressure carbon dioxide in supercritical fluid extraction and chromatography: thermodynamic analysis of the effects of helium. *Anal. Chem.* **1998**, *70*, 2104−2109.

(4) Barton, A. F. M. *CRC Handbook of Solubility Parameters and Other Cohesion Parameters*, 2nd ed.; CRC Press: Boca Raton, Florida, 1991.

(5) Allada, S. R. Solubility parameters of supercritical fluids. *Ind. Eng. Chem. Process Des. Dev.* **1984**, *23*, 344−348.

(6) Lagalante, A. F.; Hansen, B. N.; Bruno, T. J.; Sievers, R. E. Solubilities of copper(II) and chromium(III) β-diketonates in supercritical carbon dioxide. *Inorg. Chem.* **1995**, *34*, 5781−5785.

(7) Galia, A.; Muratore, A.; Filardo, G. Dispersion copolymerization of vinyl monomers in supercritical carbon dioxide. *Ind. Eng. Chem. Res.* **2003**, *42*, 448−455.

(8) Peng, D. Y.; Robinson, D. B. A new two-constant equation of state. *Ind. Eng. Chem. Fundam.* **1976**, *15*, 59−64.

(9) Wenzel, J. E.; Lanterman, H. B.; Lee, S. Experimental P-T-ρ measurements of carbon dioxide and 1,1-difluoroethene mixtures. *J. Chem. Eng. Data* **2005**, *50*, 774−776.

(10) Lora, M.; McHugh, M. A. Phase behavior and modeling of the poly(methylmethacrylate)−CO_2−methyl methacrylate system. *Fluid Phase Equilib.* **1999**, *157*, 285−297.

(11) Bae, W.; Kwon, S.; Byun, H. S.; Kim, H. Phase behavior of the poly(vinyl pyrrolidone) + N-vinyl-2-pyrrolidone + carbon dioxide system. *J. Supercrit. Fluids* **2004**, *30*,127−137.

(12) Prausnitz, J. M.; Lichtenthaler, R. N.; de Azevedo, E. G. *Molecular Thermodynamics of Fluid-Phase Equilibria*, 3rd ed.; Prentice Hall PTR: Upper Saddle River, New Jersey, 1999.

(13) Hildebrand, J. H.; Prausnitz, J. M.; Scott, R. L. *Regular and related solutions;* Van Nostrand Reinhold Co.: New York, 1970.

(14) Smart, N. G.; Carleson, T. E.; Elshani, S.; Wang, S.; Wai, C. M. Extraction of toxic heavy metals using supercritical fluid carbon dioxide containing organophosphorus reagents. *Ind. Eng. Chem. Res.* **1997**, *36*, 1819−1826.

(15) Williams, L. L.; Rubin, J. B.; Edwards, H. W. Calculation of Hansen solubility parameter values for a range of pressure and temperature conditions, including the supercritical fluid region. *Ind. Eng. Chem. Res.* **2004**, *43*, 4967−4972.

Received for review May 31, 2007. Accepted July 6, 2007. The authors thank the financial support from Università di Palermo.

JE700307R